Modeling Shock Layers in Ion-Exchange Displacement Chromatography

Venkatesh Natarajan and Steven M. Cramer
Dept. of Chemical Engineering, Rensselaer Polytechnic Institute, Troy, NY 12180

In ideal displacement chromatography (systems with infinite mass-transfer kinetics), various solutes are separated by sharp discontinuities. In real systems, however, the shocks are eroded into shock layers because of the finite rates of mass transfer. The thickness of these shock layers, which can reduce the yields achievable in these systems, depend on the flow rate, particle diameter and the ''difficulty'' of these separations. The steric mass action formalism of ion-exchange chromatography was used in concert with a solid film linear driving force model to describe the effects of flow rate, particle diameter, and the degree of difficulty of the separation on ion-exchange displacement systems. Simple pulse techniques are employed to estimate the thermodynamic and mass-transfer parameters. The simulations are then compared to experimental results over a range of conditions. The results demonstrate that this relatively simple modeling approach can be employed to describe the behavior of these nonideal displacement systems.

Introduction

Preparative ion-exchange chromatography is widely employed in the continuous and step gradient modes of operation for the purification of biomolecules (Cramer and Subramanian, 1989). In these systems, elevated salt concentrations are employed to elute the bioproduct of interest. The presence of a high salt concentration can often have a detrimental effect on the separation factor between the feed solutes, resulting in reduced yields and throughputs at high loadings.

The displacement mode of chromatography offers an attractive alternative to gradient separations. Operationally, displacement chromatography is similar to step gradient chromatography since the column is subjected to sequential stepwise changes in the inlet conditions. The column is initially equilibrated with a low ionic strength carrier buffer. The feed solution is then introduced into the column followed by a constant infusion of the displacer solution. The displacer is chosen such that it has a higher affinity for the stationary phase than the solutes in the feedstream and, thus, can effectively compete for the adsorption sites. Given sufficient column length, the displacement mode results in the feed solutes resolving into adjacent ''square-wave'' zones of highly concentrated and pure material. Once the displacer has broken through, the column is regenerated and reequilibrated with the carrier buffer. The resolving power of displacement chromatography has recently been demonstrated for a difficult protein separation (Kundu and Cramer, 1997).

In ideal systems (that is, systems with infinitely fast mass-transfer kinetics), the adjacent zones of pure material are separated by sharp discontinuities (Rhee and Amundson, 1982). However, in real systems, the finite mass-transfer rates erode the shocks into shock layers which can result in a loss of purity and yield. The shock layer represents a balance between the thermodynamic self-sharpening and the dispersive effects of nonidealities such as axial dispersion and finite mass-transfer rates (Helfferich and Carr, 1993). For a concave downward isotherm such as the Langmuir isotherm, a concentration step results in a self-sharpening wave. At a finite thickness of the shock layer, the thermodynamic self-sharpening effects and the dispersive effects balance each other (Helfferich and Carr, 1993). Thus, in displacement chromatography in real systems, the boundaries between successive bands are binary shock layers. In such a region, the concentration of one species varies rapidly from zero to its plateau concentration and that of the other varies from its plateau concentration to zero.

Correspondence concerning this article should be addressed to S. Cramer.

Rhee and coworkers (Rhee et al., 1971; Rhee and Amundson, 1972, 1974) have provided an exhaustive study of the profiles of the shock layers in single and multicomponent frontal chromatography. Zhu et al. (1993) derived a fairly straightforward analytical expression for the thickness of these layers in the case of Langmuir adsorption isotherm. Zhu and Guiochon (1994, 1995) have extended this analysis to describe the shock layer region between two adjacent solutes in a displacement train. An analytical expression was derived for the case of a Langmuir isotherm and equal Stanton and Peclet numbers for all the solutes. It turns out that in displacement systems, the thickness of the shock layer is dependent on the axial dispersion coefficient, the mass-transfer coefficient, the separation factor, and the concentration of the displacer (Zhu and Guiochon, 1994). In all these works, the transport model of choice has been the solid film linear driving force model (Guiochon et al., 1994). Such a model has also been employed in concert with the Langmuir adsorption isotherm by Phillips and coworkers (1988) to characterize transport effects in ion-exchange displacement systems.

While a more complete treatment of mass-transfer effects is provided by the general rate model (Guiochon et al., 1994), this approach entails the independent determination of several parameters. Accordingly, to simplify methods development, we will employ the solid film linear driving force model to examine the scale-up of displacement systems.

As mentioned earlier, the adsorption behavior in chromatographic systems has been traditionally described using the Langmuir isotherm. Unfortunately, this approach cannot describe the effect of the salt concentration on the adsorption behavior of the solutes in ion-exchange chromatography. Furthermore, it does not account for the multipointed nature of protein adsorption. The multivalent ion-exchange formalism has been proposed and employed successfully to describe the salt dependence of adsorption in ion-exchange systems (Cysewski et al., 1991; Velayudham and Horvath, 1988). It combines the stoichiometric displacement model (Boardman and Partridge, 1955; Kopaciewicz et al., 1983) with the electroneutrality condition to describe the ion exchange of solutes. In the case of macromolecules such as proteins, steric effects and lateral interactions are expected to play an important role (Whitley et al., 1989; Velayudhan, 1990; Brooks and Cramer, 1992; Li and Pinto, 1994). The steric mass action (SMA) model of ion-exchange chromatography incorporates the effects of salt and steric shielding on protein binding in ion-exchange systems (Brooks and Cramer, 1992). Raje and Pinto (1997) have recently shown that the steric factor in the SMA model can include both the effects of steric shielding and lateral interactions. This model has been shown to accurately predict single component and multicomponent ion-exchange chromatographic behavior in isocratic (Gallant et al., 1995a), gradient (Gallant et al., 1995b, 1996), and displacement chromatography (Gadam et al., 1995).

For systems described using the SMA model, it is not possible to derive simple analytical expressions for the shock layer profiles in displacement trains and it becomes necessary to solve the transport equations numerically. Thus, in this article, the SMA model is combined with the solid film linear driving force model to describe the behavior of displacement systems over a wide range of operating conditions.

Theory

Mass-transport equations

The solid film linear driving force model was employed in tandem with the equilibrium dispersive model to describe the effects of mass-transfer limitations in ion-exchange chromatographic systems

$$\frac{\partial C_i}{\partial \tau} + \beta \frac{\partial Q_i}{\partial \tau} + \frac{\partial C_i}{\partial x} = \frac{1}{Pe_i} \frac{\partial^2 C_i}{\partial x^2} \tag{1}$$

$$\frac{\partial Q_i}{\partial \tau} = St_i (Q_i^* - Q_i) \qquad i = 1, \ldots, NC \tag{2}$$

where Pe_i is the Peclet number and St_i is the Stanton number of the ith component, C_i and Q_i are the mobile-phase and stationary-phase concentrations of component i, and Q_i^* is the equilibrium stationary phase concentration of the ith component. The Peclet number describes the effect of axial dispersion on the system and the Stanton number is a lumped parameter describing both the external film mass-transfer resistance and the pore diffusion limitations.

The boundary conditions employed were

at $0 < \tau \le \tau_f$ and $x = 0$

$$C_i = C_{F,i} + \frac{1}{Pe_i} \frac{\partial C_i}{\partial x} \qquad i = 2, \ldots, NC-1 \tag{3}$$

$$C_{NC} = 0 \tag{4}$$

at $\tau > \tau_f$ and $x = 0$

$$C_{NC} = C_{F,NC} + \frac{1}{Pe_{NC}} \frac{\partial C_{NC}}{\partial x} \tag{5}$$

$$C_i = \frac{1}{Pe_i} \frac{\partial C_i}{\partial x} \qquad i = 2, \ldots, NC-1 \tag{6}$$

For all τ and $x = 0$

$$C_1 = C_{F,1} + \frac{1}{Pe_1} \frac{\partial C_1}{\partial x} \tag{7}$$

For all τ and $x = 1$

$$\frac{\partial C_i}{\partial x} = 0 \tag{8}$$

and the initial conditions were

for all x

$$C_i = 0 \quad \text{and} \quad Q_i = 0 \qquad i = 2, \ldots, NC \tag{9}$$

$$C_1 = C_{F,1} \quad \text{and} \quad Q_1 = \Lambda \tag{10}$$

Steric mass action formalism

The SMA formalism is a three parameter model for the description of multicomponent protein-salt equilibrium in

ion-exchange systems. The multipointed binding of the protein molecule to the stationary phase is represented as a stoichiometric exchange of mobile phase protein and bound counter ions as follows

$$C_i + \nu_i \bar{Q}_1 \Leftrightarrow Q_i + \nu_i C_1 \tag{11}$$

where ν_i is the characteristic charge of the protein, the subscript 1 represents the salt counter ion, and $\bar{Q}_1$ is the number of sites on the stationary phase available for exchange with the protein (mM). The equilibrium constant for the above reaction is given by

$$K_i = \left(\frac{Q_i}{C_i}\right)\left(\frac{C_1}{\bar{Q}_1}\right)^{\nu_i} \tag{12}$$

In addition to binding to ν_i sites, each adsorbed protein molecule will also sterically shield σ_i counter ions on the stationary phase. The number of counter ions blocked by a particular protein will be proportional to the concentration of the protein on the adsorptive surface

$$\hat{Q}_i = \sigma_i Q_i \tag{13}$$

The steric factor σ describes the nonlinear adsorption behavior of the proteins. On the other hand, the equilibrium constant K and the characteristic charge ν describe the linear adsorption behavior of the proteins.

An ion-exchange surface must maintain electroneutrality. This is given by the following equation for a multicomponent mixture

$$\Lambda = \bar{Q}_1 + \sum_{i=2}^{NC} (\nu_i + \sigma_i) Q_i \tag{14}$$

Equations 12 to 14 constitute the SMA formalism.

Unlike the Langmuirian formalism, the SMA model is a nonconstant separation factor formalism. The separation factor in the SMA formalism is a function of the salt concentration and is given by

$$\alpha_{ij} = \frac{Q_i/C_i}{Q_j/C_j} = \frac{K_i}{K_j}\left(\frac{\bar{Q}_1}{C_1}\right)^{\nu_i - \nu_j} \tag{15}$$

Since the SMA formalism is a nonconstant separation factor system, it becomes difficult to categorize the degree of difficulty of a given separation *a priori*. Equation 15 reduces to the following equation under dilute (linear) conditions

$$\alpha_{ij,\text{linear}} = \frac{K_i}{K_j}\left(\frac{\Lambda}{C_1}\right)^{\nu_i - \nu_j} \tag{16}$$

Thus, the separation factor is constant under linear conditions. Equation 16 is a measure of the closeness of the linear retention plots of solutes i and j. However, the use of this linear separation factor to quantify the degree of difficulty of separation in a nonlinear system like displacement may be inappropriate since the selectivity under nonlinear conditions may be very different.

The dynamic affinity λ of a solute for a given slope of the displacer operating line

$$\Delta\left(\equiv \frac{Q_{\text{displacer}}}{C_{\text{displacer}}}\right)$$

is defined as follows (Brooks and Cramer, 1996)

$$\lambda_i = \left(\frac{K_i}{\Delta}\right)^{1/\nu_i} \tag{17}$$

$$\alpha_{i,j}^{\text{disp}} = \frac{\lambda_i}{\lambda_j} = \frac{(K_i)^{1/\nu_i}}{(K_j)^{1/\nu_j}}(\Delta)^{(\nu_i - \nu_j)/\nu_i \nu_j} \tag{18}$$

Thus, for displacement systems, it is fit to employ the ratio of the dynamic affinities of the solutes to characterize the degree of difficulty of a separation (Shukla et al., 1988). Equation 18 defines a separation factor for displacement systems. For a given Δ, $\alpha_{i,j}^{\text{disp}}$ is constant and is a measure of the closeness of the dynamic affinities (λ) of the two solutes. The affinity ranking plot is a graphical representation of Eq. 17 and plots the logarithm of the dynamic affinity (λ) vs. the logarithm of Δ (Figure 1). Thus, it can be employed to characterize the degree of difficulty of a displacement separation.

Numerical technique

Finite difference techniques were employed to solve Eqs. 1 and 2. As the SMA isotherm is implicit, a Newton-Raphson technique was used in each step for the equilibrium calculations. The temporal terms were discretized using forward differences while the convection and diffusion terms were discretized using backward and central differences respectively.

The discretized equations were solved subject to the following stability criteria

$$\frac{\Delta c}{Pe_i(\Delta x)^2} < 0.2 \tag{19}$$

$$\frac{\Delta \tau}{\Delta x} < 1 \tag{20}$$

In the general case, the lefthand side of Eq. 19 must be less than 0.5. However, for this system, a more restrictive condition was necessary because the Newton-Raphson technique employed to solve the implicit isotherm did not tolerate negative values of the concentrations. The value of 0.2 was obtained empirically.

A FORTRAN code was written to solve the above mentioned equations. The program was run on an IBM RS/6000 workstation using IBM FORTRAN under the AIX 4.0 operating system.

Experimental Studies

Materials

Sodium monobasic phosphate, sodium dibasic phosphate, α-chymotrypsinogen A, bovine and horse cytochrome C, Nα-

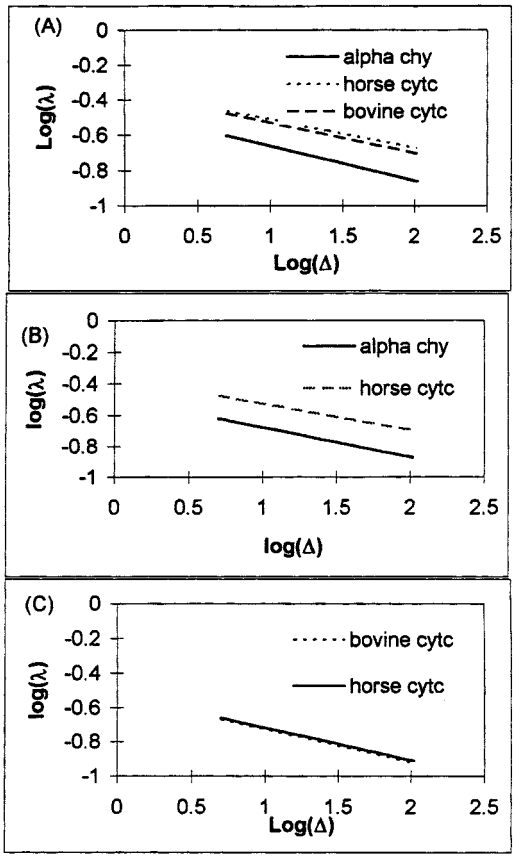

Figure 1. Affinity ranking plots for the model proteins on: (A) 8-μm Waters column; (B) 40-μm Waters column; (C) 34-μm Pharmacia HP Sepharose column.

Benzoyl-L-Arginine Ethyl Ester (BAEE), neomycin sulfate and spermine were purchased from Sigma Chemical (St. Louis, MO). Sodium chloride was purchased from Aldrich Chemical (Milwaukee, WI). O-phosphoric acid and acetonitrile were purchased from Fisher Scientific (Rochester, NY). One of the strong cation-exchange columns employed (sulfopropyl, 8 μm, 0.5×10 cm) was donated by Waters Corporation (Milford, MA). The remaining two strong cation-exchange columns were packed with Waters SP stationary phase material (sulfopropyl, 40 μm) and with Pharmacia Sepharose HP stationary phase material (SP, 34 μm), respectively. The HP Sepharose resin was a gift from Pharmacia Biotech. The strong cation-exchange column used for protein analysis (sulfopropyl, 8 μm, 0.5×5 cm) was also a gift from Waters Corporation. The POROS R/H reversed phase column (0.46 I.D.×5 cm) was obtained from PerSeptive Biosystems (Framingham, MA).

Apparatus

All displacement experiments were carried out using a Model 590 programmable HPLC pump (Waters) connected to the chromatographic columns via a Model C10W 10-port valve (Valco, Houston, TX). Data acquisition and processing were carried out using a Millenium 2010 chromatography workstation (Waters). Fractions of the column effluent were collected using an LKB 2212 Helirac fraction collector (LKB, Sweden). Protein and displacer analysis for the collected fractions were carried out using a WISP model 712 autoinjector (Waters) connected to a model 650E Advanced Protein Purification system (Waters) with a model 484 Tunable Absorbance Detector (Waters). Fluorescence absorbances were measured on a LS50B Spectrofluorometer (Perkin Elmer, Wilton, CT). UV absorbance of samples was measured on a Lambda 6 UV-Vis spectrophotometer (Perkin-Elmer).

Procedures

Estimation of SMA Parameters of Proteins. The linear SMA parameters of the proteins (K and ν) were determined using the protocols outlined by Gadam et al. (1993). Briefly, the characteristic charge and the equilibrium constant were determined using linear elution retention data at different mobile phase salt concentrations. The nonlinear parameter (σ, steric factor) was obtained from the plateau concentration of a displacement carried out at a low flow rate.

The plateau concentration is related to the steric factor by the following equation (Brooks and Cramer, 1992)

$$C_i^{\text{plateau}} = \frac{\Lambda - (C_{F,1} + \nu_{NC} C_{NC})\dfrac{1}{\lambda}}{-\nu_i\left(\dfrac{1}{\lambda} - \dfrac{\Delta}{\Omega}\right)} \tag{21}$$

$$\Omega = \frac{\nu_i}{\nu_i + \sigma_i} \tag{22}$$

Estimation of SMA Parameters of Displacers. The characteristic charge of the displacer was determined from the induced salt gradient produced from passing a front of the displacer at a known concentration. The equilibrium constant and the steric factor were then determined by a best fit of the adsorption isotherms of the displacer obtained at various mobile phase salt concentrations (Kundu, 1996).

Estimation of the Mass Transport Properties of Proteins. Pulse techniques were employed to characterize the mass transport properties of the proteins on the various stationary phases. These techniques have been employed by Arnold et al. (1985) to characterize affinity columns. The interstitial porosity was determined independently using a pulse of blue dextran and the particle porosity was computed from the elution times of the unretained protein pulses. The second moment of the elution profiles of unretained pulses (that is, protein pulses introduced into the column under high salt conditions) were employed to estimate the column plate height (HETP). The conditions for these experiments are given in Table 4a to Table 4c.

In the general rate model, the plate height equation for an unretained solute is given by (Guiochon et al., 1994)

$$\text{HETP} = \frac{2D_L}{u_o} + 2\left(\frac{(1-\epsilon_i)\epsilon_p}{\epsilon_i + (1-\epsilon_i)\epsilon_p}\right)^2\left(\frac{1}{1-\epsilon_i}\right)\left(\frac{d_p^2}{60D_p} + \frac{d_p}{6k_f}\right)u_o \tag{23}$$

The lumped mass-transfer coefficient k_m employed in the solid film linear driving force model can be related to the film mass-transfer coefficient k_f and the pore diffusion D_p as follows (Guiochon et al., 1994)

$$\frac{1}{k_m} = \epsilon_p \left(\frac{d_p^2}{60 D_p} + \frac{d_p}{6 k_f} \right) \tag{24}$$

Furthermore, the axial dispersion coefficient D_L (cm^2 min^{-1}) can be represented as follows (van Deemter et al., 1956; Arnold et al., 1985)

$$D_L = \gamma D_m + l u_o \tag{25}$$

where the first term denotes the contribution due to molecular diffusion outside the particles and the second term accounts for the eddy dispersion. In the case of proteins, the effect of the molecular diffusion term is expected to be negligible (Arnold et al., 1985). Thus, the first term in Eq. 25 can be dropped and the plate height equation becomes

$$\text{HETP} = 2l + 2 \left(\frac{(1-\epsilon_i)\epsilon_p}{\epsilon_i + (1-\epsilon_i)\epsilon_p} \right)^2 \frac{1}{(1-\epsilon_i)\epsilon_p} \frac{u_o}{k_m} \tag{26}$$

Thus, l and k_m can be obtained from the y-intercept and the slope, respectively, of Eq. 26.

To account for extra-column contributions to the HETP, pulse injections of the proteins were made under the same salt concentration with the column off-line. The HETP of the resultant peaks were then subtracted from the HETP of the protein peaks obtained with the column on-line. All the HETP data shown in the figures are the HETPs corrected for extra-column contributions.

Estimation of the Mass Transport Properties of the Displacer. The mass-transfer parameters of the displacers were obtained by a least-squares fit of the breakthrough curves of the displacers at two different flow rates. Concentrations of the displacer and the salt in these frontal runs were the same as those employed in the subsequent displacement experiments.

Displacement Experiments. The column was initially equilibrated with the carrier and then subsequently perfused with feed, displacer, and regenerant solutions. The feed load, salt concentration, and displacer concentration employed for the separation are given in the figure legends of the respective chromatograms. 200 μL fractions were collected for subsequent analysis of protein and displacer concentration in the effluent.

Protein Analysis. Analysis of the fractions collected during the displacement experiments was performed by cation-exchange HPLC under isocratic conditions. The fractions were diluted 5 to 100 fold. A mobile phase of 50 mM sodium phosphate pH 6, containing 110 mM sodium chloride, was employed for the analysis of α-chymotrypsinogen A and horse cytochrome c. For the horse and bovine cytochrome c analysis, a mobile phase of 50 mM sodium phosphate pH 6, containing 75 mM sodium chloride, was used. The proteins were detected using a UV-VIS detector at 280 nm.

Displacer Analysis. The analysis of BAEE was performed on the POROS R/H reversed-phase column after diluting the fractions 5 to 100 fold. The mobile phase employed for the analysis was 8% (v/v) acetonitrile, 0.1% (v/v) TFA and deionized water (pH 2.2).

Neomycin sulfate was analyzed using a phenol-sulfuric acid assay (Kundu et al., 1997). The fractions were diluted 5 to 20 fold. 0.8 mL of the sample was mixed with 3.2 mL of sulfuric acid, reacted for 1 min, and cooled to room temperature. 50 μL of 90% phenol (w/v) was then added and the resultant mixture was allowed to equilibrate for 30 min. The absorbance was read at 480 nm.

Spermine was analyzed by complexation with fluorescamine (Udenfriend et al., 1972; de Bernardo et al., 1974). The fractions were diluted 5 to 100 fold. A 0.28 mg/mL solution of fluorescamine in acetone was added to the fraction containing displacer in a 1:3 (v/v) ratio. Excitation at 390 nm and emission at 475 nm were then employed to quantitate the amount of displacer in the fractions.

Results and Discussion

In this article, the utility of the SMA formalism employed in concert with the solid film linear driving force model to describe the effects of flow rate, particle diameter, and separation factor on the degree of overlap in protein ion-exchange displacement systems is examined. Two model mixtures were employed: (1) α-chymotrypsinogen A-horse cytochrome c; and (2) bovine cytochrome c-horse cytochrome c. Each of these mixtures was resolved using displacement chromatography on two different particle-size materials. On each particle size, the displacements were carried out at two different flow rates. Finally, the results from these eight displacement experiments were compared with simulation results. Table 1 shows the matrix of experiments and the particle sizes and flow rates employed for each mixture.

Figures 1a to 1c are affinity ranking plots of the feed mixtures on the different stationary phase materials. As seen in these figures, the affinity lines of α-chymotrypsinogen A and horse cytochrome c (Figures 1a and 1b) are fairly wide apart while the affinity lines of bovine cytochrome c and horse cytochrome c (Figures 1a and 1c) are close together. Thus, the mixtures of α-chymotrypsinogen A and horse cytochrome c (mixture 1) and bovine cytochrome c and horse cytochrome c (mixture 2) are representative of relatively easy and difficult displacement separation problems, respectively.

Table 1. Matrix of Displacement Experiments

Feed Mixture	Stationary Phase	Column Size	Displacer	Flow Rate (mL/min)
α-Chymotrypsinogen A/ horse cytochrome c	8 μm Waters SP	0.5×10 cm	BAEE	0.2, 0.8
α-Chymotrypsinogen A/ horse cytochrome c	40 μm Waters SP	1×8 cm	Neomycin sulfate	0.8, 4
Bovine cytochrome c/ horse cytochrome c	8 μm Waters SP	0.5×10 cm	BAEE	0.2, 0.8
Bovine cytochrome c/ horse cytochrome c	34 μm Pharmacia HP SP	1×9 cm	Spermine	0.2, 1

Table 2a. SMA Parameters of Proteins and Displacers on 8-μm Waters*

Solute	ν	K	σ
α-Chymotrypsinogen A	5.14 ± 0.12	0.004	44.0 ± 4.0
Bovine cytochrome c	5.86 ± 0.06	0.0079	51.5 ± 3.2
Horse cytochrome c	6.31 ± 0.07	0.0059	54.3 ± 3.5
BAEE**	0.9 ± 0.1	9.8	0.11 ± 0.08

*Parameters obtained from Kundu (1996). $\Lambda = 590$ mM, $\epsilon = 0.7$.
**K and σ obtained from fits to isotherm data at two different salts.

Table 2b. SMA Parameters of Proteins and Displacers on 40-μm Waters*

Solute	ν	K	σ
α-Chymotrypsinogen A	5.20 ± 0.07	0.003	45 ± 3
Horse cytochrome c	6.00 ± 0.04	0.007	54 ± 2.1
Neomycin sulfate**	3.75 ± 0.31	179	3.56 ± 0.45

*$\Lambda = 525$ mM, $\epsilon = 0.725$. Experimental conditions for proteins: k' data acquired over a salt concentration range of 100–200-mM Na^+ in phosphate buffer, pH 6, flow rate 1 mL/min.
**K and σ obtained from fits to isotherm data at two different salts.

Table 2c. SMA Parameters of Proteins and Displacers on 34-μm Pharmacia HP*

Solute	ν	K	σ
Bovine cytochrome c	5.19 ± 0.07	0.00172	12.8 ± 1.5
Horse cytochrome c	5.29 ± 0.04	0.00159	10.6 ± 1.8
Spermine**	4.0 ± 0.25	0.387	0.03 ± 0.08

*$\Lambda = 1{,}200$ mM, $\epsilon = 0.85$. Experimental conditions for proteins: k' data acquired over a salt concentration range of 200–400-mM Na^+ in phosphate buffer, pH 6, flow rate 1 mL/min.
**K and σ obtained from fits to isotherm data at two different salts.

Tables 2a to 2c list the SMA parameters of the proteins and displacers employed in this study. As can be seen, the parameters of the proteins on the 8 and 40 μm Waters stationary phase are similar. This is to be expected as the chemistry, porosities, and bed capacities of the two stationary phases are similar. However, the equilibrium constant and steric factors for the Pharmacia HP stationary phase are different, which is a reflection of the different chemistry and the substantially higher bed capacity and porosity of these materials.

The steric factors of the proteins on the larger particle diameter materials were obtained using the plateau concentration of the proteins in displacement experiments carried out at low flow rates in concert with Eqs. 21 and 22. These values were then employed for the simulations at the higher flow rates. Least-squares fits to protein isotherms at two different salts had been previously employed to determine the steric factors on the 8 μm material shown in Table 2a (Kundu, 1996). Thus, these steric factors represented an average value over that range of salt concentration. Table 3 compares these values (Table 2a) to those obtained from the plateau concentrations of a displacement experiment carried out at 0.2 mL/min. As seen in the table, both approaches yield similar results. These results validate the use of isotachic concentrations in a displacement train to directly determine the steric factors of proteins. Furthermore, the good correspondence

Table 3. Comparison of Steric Factors Obtained from Least-Squares Fit to Isotherms and From Plateau Concentrations Using Eqs. 21 and 22*

Protein	Plateau Conc. (mM)	σ from Isotherm	σ from Plateau Conc.
α-Chymotrypsinogen A	0.297**	44.0	44
Bovine cytochrome c	0.467†	51.5	50
Horse cytochrome c	0.472†, 0.414**	54.3	51, 55

*System: 8-μm Waters.
**From Figure 4.
†From Figure 8.

between these approaches indicates that the average value is a reasonably good approximation over this range of salt concentration (50–150-mM Na^+) on this resin. Finally, since lateral interactions would be expected to be a function of salt concentration, these results indicate that lateral interactions may not be that important for these proteins on this stationary phase material.

The mass-transfer parameters of the proteins were obtained under unretained conditions on all the stationary phases employed in this study. The unretained elution volumes of all the proteins were identical on each stationary phase material indicating that no size exclusion occurred in these materials. Figures 2 and 3 demonstrate the techniques used to estimate the mass-transfer parameters. The stationary phase in this case was the 40-μm Waters SP material.

The second moment of the peaks was used for the computation of the HETPs of the proteins. Figure 2 shows the HETP of the two proteins as a function of the superficial mobile-phase velocity. As expected from Eq. 26, the plots are linear. The slope and y-intercept were used to calculate the lumped mass-transfer coefficient and the axial dispersion parameter, respectively.

Single component frontal chromatography was employed to determine the mass-transfer parameters of the displacer. Fractions of the column effluent were collected and analyzed for displacer concentration as described in the experimental

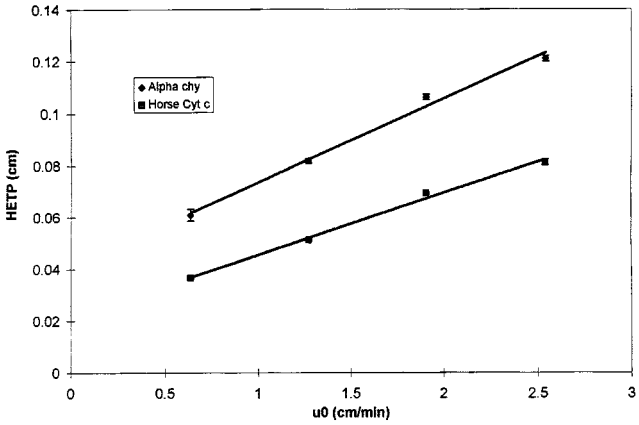

Figure 2. HETP vs. superficial velocity (u_o) for the model proteins.

Stationary phase: 40-μm Waters. Feed: pulse injections of the proteins under high salt (unretained) conditions [500-mM Na^+].

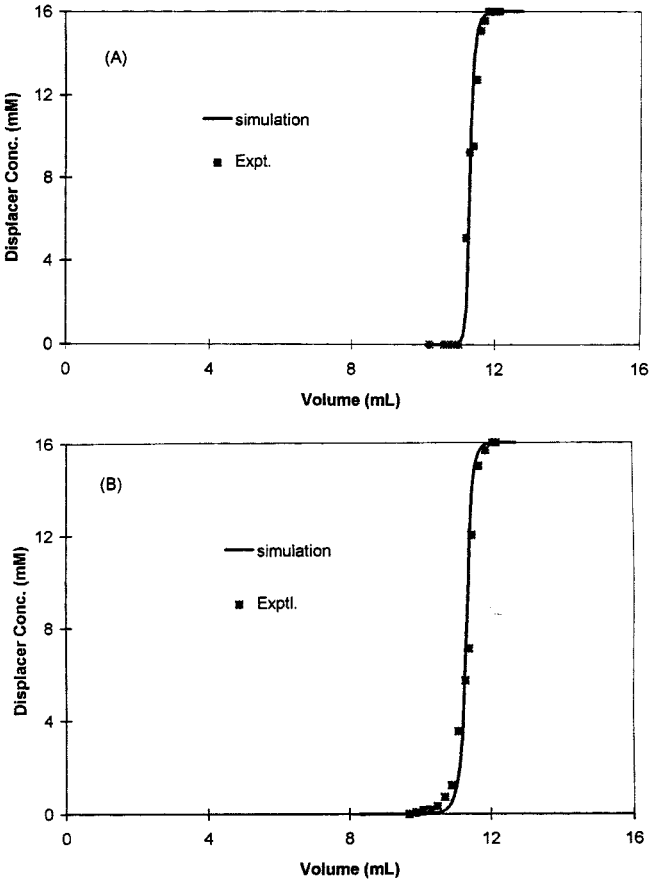

Figure 3. Experimental vs. fitted breakthrough curves.

Stationary phase: 40-μm Waters. Feed: 16-mM neomycin sulfate; salt = 30 mM; pH = 6. (A) 0.8 mL/min, (B) 4 mL/min.

section. Figure 3 shows the experimental data points of the single component frontals of neomycin sulfate at two different flow rates and the corresponding least-squares fit of the data using Eqs. 1 and 2. These frontal experiments were carried out under the same displacer and salt concentrations employed in the subsequent displacement experiments. The mass transport parameters l and k_m obtained at 0.8 and 4 mL/min were 0.04 and 41 and 0.04 and 39, respectively. Since these parameters were within 5% of each other, an average value of these parameters was used as given in Table 4d.

As seen in the figures, the beginning of the displacer front is not very well fit at the higher flow rate (Figure 3b). However, as will be shown below, this discrepancy has minimal effect on predicting the behavior of the displacement separations.

The mass-transport parameters of the proteins and displacers on the remaining stationary phases were obtained in a similar fashion.

Tables 4a to 4c list the values of the mass-transfer parameters (the axial dispersion parameter l and the lumped mass-transfer coefficient k_m) of the proteins and the displacers on the various stationary phases. A stationary phase possesses good transport properties if it has a low l and a high k_m. As expected, the 8 μm Waters stationary phase possessed the best transport properties. The lumped mass-transport parameter (k_m) on the 8 μm particles is approximately 8 to 10 times higher than on the 40 μm particles. Interestingly, the 34 μm Pharmacia stationary phase has a k_m which is roughly 3 times higher than that on the 40 μm Waters phase, indicating superior mass-transfer properties.

Although the axial dispersion parameter (l) is lower on the 8 μm particles than on the 40 μm particles, the difference is not as dramatic as seen for k_m. Further, the value of l is lower on the 34 μm Pharmacia particles than both of the Waters materials.

The transport parameters of the displacers are given in Table 4d. As described above, these parameters were obtained by fitting frontal chromatography experiments under various experimental conditions. Thus, one cannot compare the mass-transfer parameters of the different displacers.

Having obtained the necessary parameters, it is now possible to simulate displacement experiments over a wide range of conditions.

Table 4a. Mass-Transport Parameters of Proteins on 8-μm Waters*

Protein	l (cm)	Slope	k_m (min^{-1})
α-Chymotrypsinogen A	0.0116 ± 0.0004	0.0031 ± 0.0001	264
Bovine cytochrome c	0.0109 ± 0.0006	0.0027 ± 0.0002	302
Horse cytochrome c	0.0106 ± 0.0008	0.0027 ± 0.0002	302

*$\epsilon_{inter} = 0.5$, $\epsilon_{pore} = 0.4$. Experimental conditions: 800-mM Na^+ in phosphate buffer, pH 6.

Table 4b. Mass-Transport Parameters of Proteins on 40-μm Waters*

Protein	l (cm)	Slope	k_m (min^{-1})
α-Chymotrypsinogen A	0.041 ± 0.004	0.032 ± 0.002	27
Horse cytochrome c	0.022 ± 0.002	0.0237 ± 0.001	36

*$\epsilon_{inter} = 0.5$, $\epsilon_{pore} = 0.45$. Experimental conditions: 800-mM Na^+ in phosphate buffer, pH 6.

Table 4c. Mass-Transport Parameters of Proteins on 34-μm Pharmacia HP*

Protein	l (cm)	Slope	k_m (min^{-1})
Bovine cytochrome c	0.0067 ± 0.0003	0.0122 ± 0.0002	102
Horse cytochrome c	0.0071 ± 0.0004	0.0122 ± 0.0003	102

*$\epsilon_{inter} = 0.4$, $\epsilon_{pore} = 0.75$. Experimental conditions: 1-M Na^+ in phosphate buffer, pH 6.

Table 4d. Mass-Transport Parameters of Displacers*

Displacer	Stationary Phase	l (cm)	k_m (min^{-1})
BAEE	8-μm Waters	0.005	450
Neomycin sulfate	40-μm Waters	0.04	40
Spermine	34-μm Pharmacia HP	0.0112	80

*These were obtained by fitting simulations to experimental frontal data. The salt counter-ion employed in the study was Na^+. An l of 10^{-4} cm and a k_m of 500 min^{-1} was assumed for the simulations.

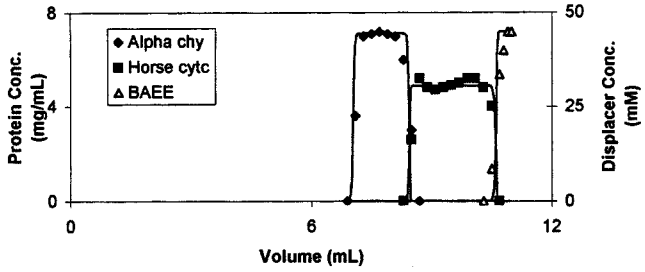

Figure 4. Experimental vs. simulated displacement profiles: feed, 1.8 mL of 0.23-mM α-chymotrypsinogen A and 0.53-mM horse cytochrome c in 50-mM Na^+ (pH = 6); flow rate, 0.2 mL/min.

Stationary phase: 8-μm Waters SP strong cation exchanger. Displacer: 45-mM BAEE. Solid lines represent simulation results.

Figures 4 and 5 compare the experimental and simulated results of the displacements of α-chymotrypsinogen A and horse cytochrome c on the 8 μm Waters material at 0.2 and 0.8 mL/min, respectively. As seen in the figures, the flow rate had a marginal effect on this separation. This is to be expected since the separation is relatively easy (Figure 1a). Further, the simulations do a good job of predicting the effect of the flow rate on the degree of overlap in these separations. The yields at $\geq$ 95% purity for both the experiments and the simulations are given in Table 5. As seen in the table, the experimental and simulated yields are in close agreement for this separation.

Figures 6 and 7 compare the experimental and simulated results of the displacements of α-chymotrypsinogen A and horse cytochrome c on the 40 μm Waters stationary phase at 0.8 and 4 mL/min, respectively. The effect of the flow rate is more pronounced in this case. At the lower flow rate (Figure 6), the linear velocity is the same as in Figure 4, however, the degree of overlap is higher. This is due to the fact that the k_m on this stationary phase material is approximately an order of magnitude lower than on the 8 μm resin (Tables 4a and 4b). At the higher flow rate, the degree of overlap is further increased. Again, the simulated and experimental yields of the proteins were in close agreement (Table 6). These

Table 5. Experimental vs. Simulated Yields at $\geq$ 95% Purity: System, α-Chymotrypsinogen A/Horse Cytochrome c on 8-μm Waters Column

Protein	Experimental Yield (%)	Simulated Yield (%)
Flow rate = 0.2 mL/min		
α-Chymotrypsinogen A	100.0	99.9
Horse cytochrome c	92.7	96.7
Flow rate = 0.8 mL/min		
α-Chymotrypsinogen A	98.4	99.9
Horse cytochrome c	90.1	93.9

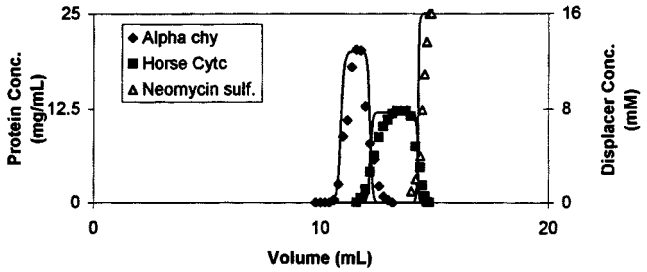

Figure 6. Experimental vs. simulated displacement profiles: feed, 3.7 mL of 0.27-mM α-chymotrypsinogen A and 0.51-mM horse cytochrome c in 30-mM Na^+ (pH = 6); flow rate, 0.8 mL/min.

Stationary phase: 40-μm Waters SP strong cation exchanger. Displacer: 16-mM neomycin sulfate. Solid lines represent simulation results.

results indicate that lower flow rates are required when carrying out displacement separations on large particle diameter materials.

The displacement described above involved the relatively easy separation of the α-chymotrypsinogen A from horse cytochrome c. As shown in Figures 1a and 1c, the separation of bovine cytochrome c from horse cytochrome c is significantly more difficult. Figures 8 and 9 compare the experimental and simulated results of the displacements of bovine cytochrome c and horse cytochrome c on the 8 μm Waters stationary

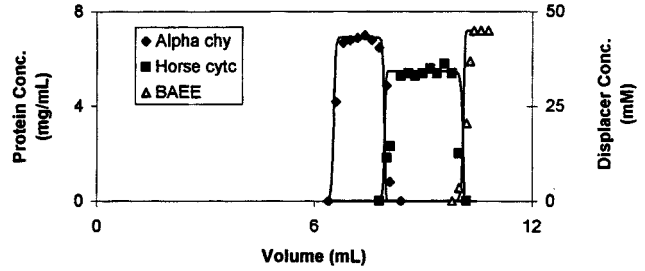

Figure 5. Experimental vs. simulated displacement profiles: feed, 1.8 mL of 0.23-mM α-chymotrypsinogen A and 0.53-mM horse cytochrome c in 50-mM Na^+ (pH = 6); flow rate, 0.8 mL/min.

Stationary phase: 8-μm Waters SP strong cation exchanger. Displacer: 45-mM BAEE. Solid lines represent simulation results.

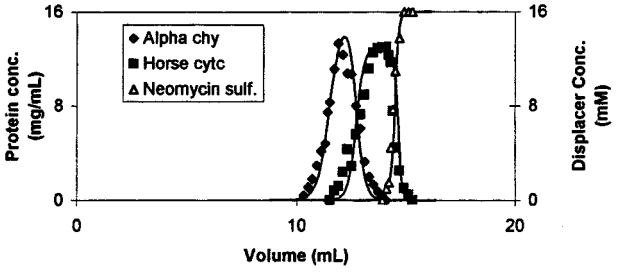

Figure 7. Experimental vs. simulated displacement profiles: feed, 3.7 mL of 0.27-mM α-chymotrypsinogen A and 0.51-mM horse cytochrome c in 30-mM Na^+ (pH = 6); flow rate, 4.0 mL/min.

Stationary phase: 40 μm-Waters SP strong cation exchanger. Displacer: 16-mM neomycin sulfate. Solid lines represent simulation results.

Table 6. Experimental vs. Simulated Yields at ≥ 95% Purity: System, α-Chymotrypsinogen A/Horse Cytochrome c on 40-μm Waters Column

Protein	Experimental Yield (%)	Simulated Yield (%)
Flow rate = 0.8 mL/min		
α-Chymotrypsinogen A	97.0	96.0
Horse cytochrome c	87.1	92.4
Flow rate = 4.0 mL/min		
α-Chymotrypsinogen A	51.3	51.5
Horse cytochrome c	36.0	36.4

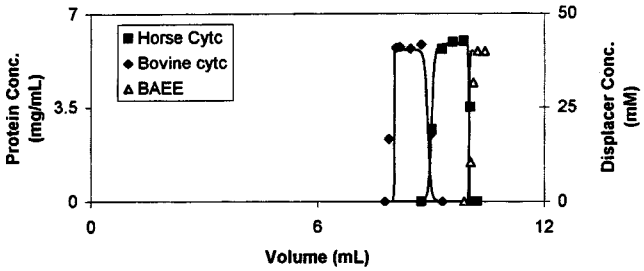

Figure 8. Experimental vs. simulated displacement profiles: feed, 0.8 mL of 0.51-mM bovine cytochrome c and 0.51-mM horse cytochrome c in 50-mM Na^+ (pH = 6); flow rate, 0.2 mL/min.

Stationary phase: 8-μm Waters SP strong cation exchanger. Displacer: 40-mM BAEE. Solid lines represent simulation results.

phase at 0.2 and 0.8 mL/min, respectively. While both of these displacement experiments resulted in good separations, the effect of the flow rate was more pronounced than seen for the α-chymotrypsinogen A and horse cytochrome c separation on the same stationary phase (Figures 4 and 5). This is to be expected since the separation is more difficult. Again, the simulations capture the salient features of the separations and the experimental and predicted yields are in close agreement (Table 7).

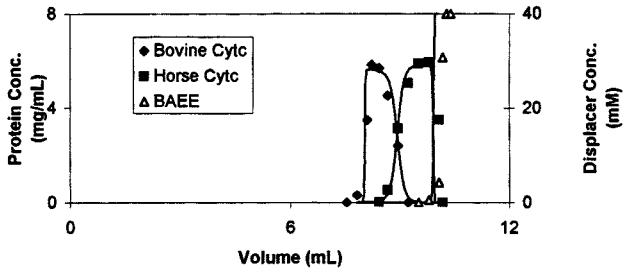

Figure 9. Experimental vs. simulated displacement profiles: feed, 0.8 mL of 0.51-mM bovine cytochrome c and 0.51-mM horse cytochrome c in 50-mM Na^+ (pH = 6); flow rate, 0.8 mL/min.

Stationary phase: 8-μm Waters SP strong cation exchanger. Displacer: 40-mM BAEE. Solid lines represent simulation results.

Table 7. Experimental vs. Simulated Yields at ≥ 95% Purity: System, Bovine Cytochrome c/Horse Cytochrome c on 8-μm Waters Column

Protein	Experimental Yield (%)	Simulated Yield (%)
Flow rate = 0.2 mL/min		
Bovine cytochrome c	92.2	94.3
Horse cytochrome c	83.2	88.9
Flow rate = 0.8 mL/min		
Bovine cytochrome c	88.7	83.6
Horse cytochrome c	70.3	73.1

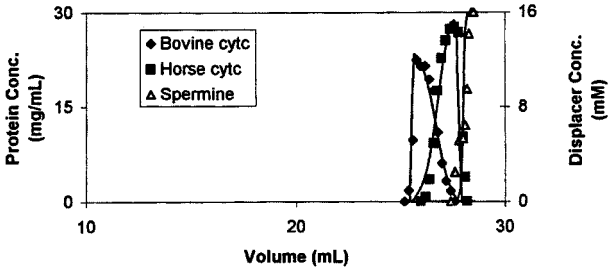

Figure 10. Experimental vs. simulated displacement profiles: feed, 4.2 mL of 0.53-mM bovine cytochrome c and 0.55-mM horse cytochrome c in 50-mM Na^+ (pH = 6); flow rate, 0.2 mL/min.

Stationary phase: 34 μm Pharmacia HP SP strong cation exchanger. Displacer: 16-mM spermine. Solid lines represent simulation results.

The separation of the two cytochrome c's was also carried out using the 34 μm Pharmacia stationary phase at 0.2 and 1 mL/min, respectively. As seen in Figure 10, at low flow rates some separation was achieved under these displacement conditions. In fact, the separation could be readily improved by increasing the loading and/or decreasing the displacer concentration. The simulation for this separation (Figure 10) captures the general behavior of this separation; however, it underpredicts the yield of bovine cytochrome c (Table 8). When this displacement is carried out at 1 mL/min, there is essentially no separation at all (Figure 11). Clearly, for very difficult separations on larger particle diameter systems, low flow rates are required. While the simulation does a good job of predicting this behavior, the degree of tailing of the pro-

Table 8. Experimental vs. Simulated Yields at ≥ 95% Purity: System, Bovine Cytochrome c/Horse Cytochrome c on 34-μm Pharmacia Column

Protein	Experimental Yield (%)	Simulated Yield (%)
Flow rate = 0.2 mL/min		
Bovine cytochrome c	71.0	57.2
Horse cytochrome c	0.0	0.0
Flow rate = 1.0 mL/min		
Bovine cytochrome c	0.0	0.0
Horse cytochrome c	0.0	0.0

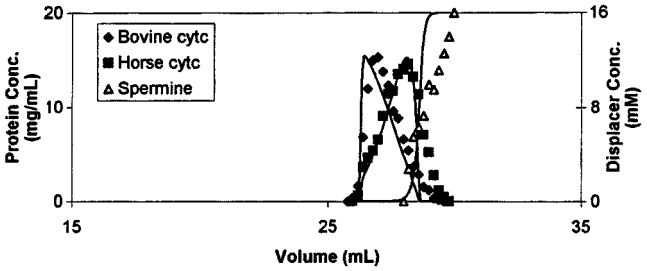

Figure 11. Experimental and simulated displacement profiles: feed, 4.2 mL of 0.53-mM bovine cytochrome c and 0.55-mM horse cytochrome c in 50-mM Na^+ (pH = 6); flow rate, 1.0 mL/min.

Stationary phase: 34 μm Pharmacia HP SP strong cation exchanger. Displacer: 16-mM spermine. Solid lines represent simulation results.

tein profiles into the displacer zone was underpredicted. It may be that the relatively straightforward parameter estimation technique is not sufficient for this resin and that other modes of transport (such as surface diffusion, kinetics of adsorption/desorption) may be affecting this separation.

Conclusions

In this article we have demonstrated that the lumped mass-transport model can be employed in concert with the SMA formalism of ion exchange to accurately describe the effects of flow rate, particle size and the degree of difficulty of the separation on the yields obtainable in ion-exchange displacement systems. The parameters required to characterize the linear thermodynamic behavior and mass-transport properties of the system can be readily obtained from simple pulse experiments.

In all the cases described above, the simulations captured the salient features of the displacement experiments. The utility of this approach for studying the optimization of nonideal, nonlinear chromatographic systems in general will be the subject of a future report.

Acknowledgments

This research has been funded by grant No. CTS-9416921 from the National Science Foundation.

Notation

C = mobile phase concentration, mM
C_F = feed concentration, mM
k' = capacity factor, dimensionless
L = length of column, cm
NC = number of components in the system
Pe = Peclet number = Lu/D
Q = stationary phase concentration (= mmol adsorbed/mL solid phase), mM
Q^* = stationary phase concentration at equilibrium with C, mM
$\hat{Q}_1$ = concentration of bound salt which is sterically shielded, mM
St = Stanton number = $k_m L/u$
t = time, min
t_o = time taken for an inert tracer to traverse the column, min
u = chromatographic velocity = u_o/ϵ, cm·min^{-1}
u_o = superficial velocity, cm·min^{-1}
x = axial distance along column
α = separation factor
β = phase ratio = $(1-\epsilon)/\epsilon$
ϵ = total porosity
ϵ_{inter} = interstitial porosity
ϵ_{pore} = particle porosity
τ = dimensionless time = t/t_o
τ_f = dimensionless feed time
Λ = bed capacity, mM

Subscripts

i = component number: $i = 1$ is salt counterion; i = NC is displacer
j = spatial index
n = temporal index

Literature Cited

Arnold, F. H., H. W. Blanch, and C. R. Wilke, "Analysis of Affinity Separations: II. The Characterization of Affinity Columns by Pulse Techniques," *Chem. Eng. J.*, **30**, B25 (1985).

Boardman, N. K., and S. M. Partridge, "Separation of Neutral Proteins on Ion Exchange Resins," *Biochem. J.*, **59**, 543 (1955).

Brooks, C. A., and S. M. Cramer, "Steric Mass-Action Ion Exchange: Displacement Profiles and Induced Salt Gradients," *AIChE J.*, **38**, 1969 (1992).

Brooks, C. A., and S. M. Cramer, "Solute Affinity in Ion Exchange Displacement Chromatography," *Chem. Eng. Sci.*, **51**, 3847 (1996).

Cramer, S. M., and G. Subramaniam, "Preparative Liquid Chromatography of Biomolecules—New Directions," *New Directions in Sorption Technology*, E. G. Keller and R. T. Yang, eds., Butterworth, Stoneham, U.K. (1989).

Cysewski, P., A. Jaulmes, R. Lemque, B. Sebille, C. Vidal-Madjar, and G. Jilge, "Multivalent Ion Exchange Model of Biopolymer Chromatography for Mass Overload Conditions," *J. Chromatog.*, **548**, 61 (1991).

de Bernardo, S., M. Weigele, V. Toome, K. Manhart, and W. Leimgruber, "Studies on the Reaction of Fluorescamine with Primary Amines," *Arch. Biochem. Biophy.*, **163**, 390 (1974).

Gadam, S. D., G. Jayaraman, and S. M. Cramer, "Characterization of Non-Linear Adsorption Properties of Dextran-Based Polyelectrolyte Displacers in Ion-Exchange Systems," *J. Chromatog.*, **630**, 37 (1993).

Gadam, S. D., S. R. Gallant, and S. M. Cramer, "Transient Profiles in Ion Exchange Displacement Chromatography," *AIChE J.*, **41**, 1676 (1995).

Gallant, S. R., A. Kundu, and S. M. Cramer, "Modeling Non-Linear Elution of Proteins in Ion-Exchange Chromatography," *J. Chromatog. A*, **702**, 125 (1995a).

Gallant, S. R., A. Kundu, and S. M. Cramer, "Optimization of Step Gradient Separations: Consideration of Nonlinear Adsorption," *Biotechnol. & Bioeng.*, **47**, 355 (1995b).

Gallant, S. R., S. Vunnum, and S. M. Cramer, "Optimization of Preparative Ion Exchange Chromatography of Proteins: Linear Gradient Separations," *J. Chromatog. A*, **725**, 295 (1996).

Guiochon, G., S. G. Shirazi, and A. M. Katti, *Fundamentals of Preparative and Nonlinear Chromatography*, Academic Press, New York (1994).

Helfferich, F. G., and P. W. Carr, "Non-Linear Waves in Chromatography: I. Waves, Shocks, and Shapes," *J. Chromatog.*, **629**, 97 (1993).

Kopaciewicz, W., M. A. Rounds, J. Fausnaugh, and F. E. Regnier, "Retention Model for High-Performance Ion Exchange Chromatography," *J. Chromatog.*, **266**, 3 (1983).

Kundu, A., "Low Molecular Weight Displacers for Protein Purification in Ion Exchange Systems," PhD Diss., Rensselaer Polytechnic Inst., Troy, NY (1996).

Kundu, A., A. A. Shukla, K. A. Barnthouse, J. Moore, and S. M. Cramer, "Displacement Chromatography of Proteins Using Sucrose Octasulfate," *BioPharm*, **10**, 64 (1997).

Kundu, A., and S. M. Cramer, "Low-Molecular-Weight Displacers for High-Resolution Protein Separations," *Anal. Biochem.*, **248**, 1 (1997).

Li, Y.-L., and N. G. Pinto, "Influence of Lateral Interactions on

Preparative Protein Chromatography: I. Isotherm Behavior,'' *J. Chromatog. A*, **658**, 445 (1994).
Phillips, M. W., G. Subramanian, and S. M. Cramer, ''Theoretical Optimization of Operating Parameters in Non-Ideal Displacement Chromatography,'' *J. Chromatog.*, **454**, 1 (1988).
Raje, P., and N. G. Pinto, ''Combination of the Steric Mass Action and Non-Ideal Surface Solution Models for Overload Protein Ion-Exchange Chromatography,'' *J. Chromatog. A*, **760**, 89 (1997).
Rhee, H.-K., B. F. Bodin, and N. R. Amundson, ''A Study of the Shock Layer in Equilibrium Exchange Systems,'' *Chem. Eng. Sci.*, **26**, 1571 (1971).
Rhee, H.-K., and N. R. Amundson, ''A Study of the Shock Layer in Nonequilibrium Exchange Systems,'' *Chem. Eng. Sci.*, **27**, 199 (1972).
Rhee, H.-K., and N. R. Amundson, ''Shock Layer in Two Solute Chromatography: Effect of Axial Dispersion and Mass Transfer,'' *Chem. Eng. Sci.*, **29**, 2049 (1974).
Rhee, H.-K., and N. R. Amundson, ''Analysis of Multicomponent Separation by Displacement Development,'' *AIChE J.*, **28**, 423 (1982).
Shukla, A. A., K. A. Barnthouse, S. S. Bae, J. A. Moore, and S. M. Cramer, ''Structural Characteristics of Low Molecular Mass Displaces for Cation Exchange Chromatography,'' *J. Chromatog. A*, **814**, 83 (1998).
Udenfriend, S., S. Stein, P. Bohlen, and W. Dairman, ''Fluorescamine: A Reagent for Assay of Amino Acids, Peptides, Proteins, and Primary Amines in the Picomole Range,'' *Science*, **178**, 871 (1972).
van Deemter, J. J., F. J. Zuiderweg, and A. Klinkerberg, ''Longitudinal Diffusion and Resistance to Mass Transfer as Causes of Nonideality in Chromatography,'' *Chem. Eng. Sci.*, **5**, 271 (1956).
Velayudhan, A., and Cs. Horvath, ''Preparative Chromatography of Proteins. Analysis of the Multivalent Ion Exchange Formalism,'' *J. Chromatog.*, **443**, 13 (1988).
Velayudhan, A., ''Studies in Nonlinear Chromatography,'' PhD Diss., Yale University, New Haven, CT (1990).
Whitley, R. D., R. Wachter, F. Liu, and N.-H. L. Wang, ''Ion Exchange Equilibria of Lysozyme, Myoglobin, and Bovine Serum Albumin,'' *J. Chromatog.*, **465**, 137 (1989).
Zhu, J., Z. Ma, and G. Guiochon, ''The Thickness of Shock Layers in Liquid Chromatography,'' *Biotechnol. Prog.*, **9**, 421 (1993).
Zhu, J., and G. Guiochon, ''Shock Layer Thickness and Optimum Linear Velocity in Displacement Chromatography,'' *J. Chromatog.*, **659**, 15 (1994).
Zhu, J., and G. Guiochon, ''Production Rate of an Isotachic Train in Displacement Chromatography,'' *AIChE J.*, **41**, 45 (1995).

Manuscript received May 21, 1998, and revision received Sept. 23, 1998.